Title	Enabling Wireless Power Transfer in Cellular Networks: Architecture, Modeling and Deployment
Author(s)	Huang, K; Lau, VKN
Citation	IEEE Transactions on Wireless Communications, 2014, v. 13 n. 2, p. 902-912
Issued Date	2014
URL	http://hdl.handle.net/10722/200611
Rights	IEEE Transactions on Wireless Communications. Copyright © IEEE.

Enabling Wireless Power Transfer in Cellular Networks: Architecture, Modeling and Deployment

Kaibin Huang and Vincent K. N. Lau

***Abstract*—*Microwave power transfer* (MPT) delivers energy wirelessly from stations called *power beacons* (PBs) to mobile devices by microwave radiation. This provides mobiles practically infinite battery lives and eliminates the need of power cords and chargers. To enable MPT for mobile recharging, this paper proposes a new network architecture that overlays an uplink cellular network with randomly deployed PBs for powering mobiles, called a *hybrid network*. The deployment of the hybrid network under an outage constraint on data links is investigated based on a stochastic-geometry model where single-antenna base stations (BSs) and PBs form independent homogeneous Poisson point processes (PPPs) with densities λ_b and λ_p, respectively, and single-antenna mobiles are uniformly distributed in Voronoi cells generated by BSs. In this model, mobiles and PBs fix their transmission power at p and q, respectively; a PB either radiates isotropically, called *isotropic MPT*, or directs energy towards target mobiles by beamforming, called *directed MPT*. The model is used to derive the tradeoffs between the network parameters $(p, \lambda_b, q, \lambda_p)$ under the outage constraint. First, consider the deployment of the cellular network. It is proved that the outage constraint is satisfied so long as the product $p\lambda_b^{\frac{\alpha}{2}}$ is above a given threshold where α is the path-loss exponent. Next, consider the deployment of the hybrid network assuming infinite energy storage at mobiles. It is shown that for isotropic MPT, the product $q\lambda_p\lambda_b^{\frac{\alpha}{2}}$ has to be above a given threshold so that PBs are sufficiently dense; for directed MPT, $z_m q\lambda_p\lambda_b^{\frac{\alpha}{2}}$ with z_m denoting the array gain should exceed a different threshold to ensure short distances between PBs and their target mobiles. Furthermore, similar results are derived for the case of mobiles having small energy storage.**

***Index Terms*—Power transmission, cellular networks, energy harvesting, stochastic processes, adaptive arrays, mobile communication.**

I. Introduction

ONE of the most desirable new features for mobile devices is wireless recharging that eliminates the need of power cords and chargers. To realize this feature, the paper proposes a novel network architecture (see Fig. 1) where stations called *power beacons* (PBs) are deployed in an existing cellular network for recharging mobiles and sensors via microwave radiation known as *microwave power transfer* (MPT). The challenges in realizing wireless recharging by MPT are threefold, namely creating *line-of-sight* (LOS) links from PBs to mobiles to enable close-to-free-space power transfer, forming sharp energy beams at PBs to counteract propagation loss, and reducing power consumption of mobiles. These challenges can be tackled by the advancements of three technologies, respectively. First, PBs require neither backhaul links nor complex computation, allowing low-cost and dense deployment at flexible locations with connections to the electrical grid e.g., walls and lamp poles. Second, massive antenna arrays with tens to hundreds of elements are a technology currently under active development [1] and can be used at PBs for forming sharp energy beams towards mobiles to achieve the MPT efficiency close to one. Last, the ongoing deployment of *small-cell networks* [2] and the advancements in low-power electronics will substantially reduce the required transmission power of mobiles. Consequently, PBs with a practical density can deliver sufficient power for mobile recharging.

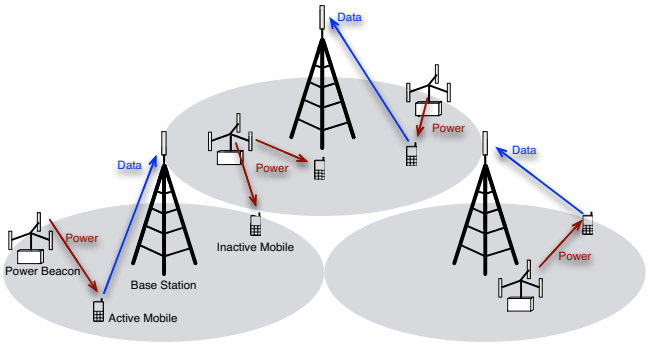

Fig. 1. Hybrid network that overlays an uplink cellular network with randomly deployed power beacons wirelessly recharging mobiles via microwave radiation.

In this paper, an uplink cellular network overlaid with PBs, called the *hybrid network*, is studied using a stochastic-geometry model where *base stations* (BSs) and PBs form independent homogeneous *Poisson point processes* (PPPs) and mobiles are uniformly distributed in corresponding Voronoi cells with respect to BSs [3]. In the model, PBs power uplink transmissions by either isotropic radiation or beamforming towards target mobiles, called *isotropic* or *directed* MPT, respectively. The model is used to derive the tradeoffs between the network parameters including the PB/mobile transmission power and PB/BS densities for different network configurations accounting for isotropic/directed MPT and mobiles having large/small energy storage. The results provide insight into the hybrid-network deployment and throughput.

A. Microwave Power Transfer

Wireless power transfer is usually implemented in practice based on one of the three different technologies, namely inductive coupling [4], magnetic resonance coupling [5], and

Manuscript received April 26, 2013; revised August 18 and November 1, 2013; accepted November 2, 2013. The associate editor coordinating the review of this paper and approving it for publication was T. J. Lim.

K. Huang is with the Department of Electrical and Electronic Engineering, the University of Hong Kong, Pok Fu Lam, Hong Kong (e-mail: huangkb@ieee.org).

V. K. N. Lau is with the Department of Electrical and Computer Engineering, the Hong Kong University of Science and Technology, Clear Water Bay, Hong Kong (e-mail: eeknlau@ece.ust.hk).

Digital Object Identifier 10.1109/TWC.2013.122313.130727

TABLE I
SUMMARY OF NOTATION

Symbol	Meaning
Φ, λ_b	PPP of base stations, density of Φ
Ψ, λ_p	PPP of PBs, density of Ψ
Y_0, U_0, T_0	Typical base station, mobile and PB
U_Y	Mobile served by base station Y
G_{XY}	Fading coefficient for the channel from transmitter Y to receiver X
α, β	Path-loss exponent for a data channel, a MPT channel
P_{out}, ϵ	Outage probability and its maximum for the typical base station
p, q	Transmission power for mobiles, PBs
ω	Duty cycle for mobile transmission
d_0, s_0	Reference distance, path loss at this distance for the propagation model
ν	Parameter of the MPT propagation model
θ	SINR threshold for outage events
$\mathcal{C}$	Set of base stations serving mobiles whose interference to Y_0 is canceled
δ	The maximum power-outage probability for the case of mobiles having small energy storage
$\mathbb{R}_+$	Set of nonnegative numbers
K	Number of interfering mobiles each BS cancels

MPT [6] corresponding to short range (tens of centi-meters), mid range (several meters), and long range (up to tens of kilometers), respectively. Besides limited transfer distances, both inductive and magnetic-resonance coupling require alignment and calibration of coils at transmitters and receivers, making these technologies unsuitable for mobile recharging.

MPT has no such limitations but suffers from potentially severe propagation loss over long transfer distances. Such loss can be overcome by free-space beaming and intercepting microwave energy using antennas with large apertures. Based on this principle, efficient point-to-point MPT over long distances has been demonstrated in experiments of MPT powered helicopters [7] or airplanes [8], [9] and the design of solar-power satellites [10]. Large antennas with the dimensions in the aforementioned experiments are impractical and unnecessary for MPT in the hybrid network where efficient MPT relies on deploying dense PBs to shorten power-transfer distances.

Recently, *simultaneous wireless information-and-power transfer* (SWIPT) has emerged to be a new research area, which traditionally was treated as two separate problems [11]–[14]. The seamless integration of the two types of transfers both using microwaves will lead to practical solutions for MPT. In [11], [12], the authors investigated the information capacity of a point-to-point wireless channel under the constraint that the average received power is above a given threshold, establishing the tradeoff between the transferred power and information rate over the same channel. The novel problem formulation has motivated a series of extension where the said tradeoff is optimized for more complex SWIPT systems including multiple-input-multiple-output (MIMO) broadcast channels [14], [15], two-way channels [16], relay assisted communication [17], and broadband channels [18], [19]. Different from prior work, this paper considers coupled wireless power and information transfer in a large-scale network and the resultant relation between the hybrid-network parameters can be interpreted as the network counterparts of the existing capacity-and-power tradeoffs for small-scale systems.

B. Modelling the Access and Power-Beacon Networks

Cellular networks traditionally are modelled using hexagonal grids but such models lack tractability and fail to account for ad hoc BS deployment that is a trend of network evolution [2]. These drawbacks can be overcome by using stochastic geometry for modeling the cellular-network architecture [20]–[23]. In [20], a cellular network was modeled as a bivariate PPP that comprises two independent PPPs representing BSs and mobiles, respectively. As a result, the cellular network is distributed as a Poisson Voronoi tessellation. This random network model was applied in [21] to study the economics of cellular networks, and combined with a channel-fading model to study the downlink coverage in [22] and uplink coverage in [23], yielding analytical results consistent with the performance of practical networks. An uplink network is considered in this paper where single-antenna mobiles transmit data to single-antenna BSs under an outage-probability constraint for a target received signal-to-interference-and-noise ratio (SINR). Aligned with existing approaches, BSs in the uplink network is modeled as a homogeneous PPP with density λ_b and each cell of the resultant Voronoi tessellation comprises a uniformly distributed active mobile. Data links are characterized by both path loss and fading with a general distribution.

Mobiles in the current cellular-network model are powered by MPT rather than reliable power supplies assumed in prior work. Randomly deployed PBs are modeled as a homogeneous PPP similar to the existing models of mobile ad hoc networks (MANETs) (see e.g., [24]). MPT uses frequencies outside the data bandwidth (e.g., in the ISM band) and hence causes no interference to uplink transmissions. The PB transmission power is assumed to spread over sufficiently large bandwidth so that the power-spectrum density meets regulations on microwave radiation. MPT links have path loss but no fading due to relatively short propagation distances. Mobiles intercept energy transferred from PBs continuously and store it for powering subsequent uplink transmission.

The current approach is similar to that in [25] as both apply stochastic geometry to model and design energy-harvesting networks. However, the current work focuses on a new network architecture different from a MANET in [25], leading to a set of novel results and insight. To be specific, mobiles in the current model communicate with randomly located BSs and hence transmission distances vary instead of being fixed as a constant in the MANET model in [25]. Furthermore, in the

current model, the received power at each mobile is a function of the PB process, which introduces the tradeoff between the parameters of the PB and the BS processes. In contrast, such a tradeoff is irrelevant in the MANET model in [25] where the energy-arrival processes at mobiles are modeled as *independent and identically distributed* (i.i.d.) sequences.

Following the initial version of this work, a similar stochastic-geometry model has been developed in [26] for cognitive radio networks where transmitters in a secondary network power their transmissions by harvesting energy from a primary network. Given the primary network, the transmission capacity for the secondary network has been characterized and optimized over the node density and transmission power.

C. Contributions and Organization

Let λ_p and λ_b denote the PB and BS densities, respectively. The transmission power of a mobile is represented by p and that of a PB by q. The constants α and β are the path-loss exponents for data and MPT links, respectively. Moreover, $\{c_n\}$ are a set of constants to be derived in the sequel. The notation is summarized in Table I.

The main contributions of the paper are summarized as follows.

1) Consider the deployment of the cellular network. Define the *feasibility region* $\mathcal{F}_c$ as all feasible combinations of the network parameters (p, λ_b) under the outage constraint. It is proved that

$$\mathcal{F}_c = \left\{(p, \lambda_b) \in \mathbb{R}_+^2 \mid p\lambda_b^{\frac{\alpha}{2}} \geq c_1\right\}.$$

It is observed that the minimum p increases with decreasing λ_b and vice versa.

2) Consider the deployment of the hybrid network. Define the corresponding feasibility region $\mathcal{F}_h$ as all combinations of $(q, \lambda_p, \lambda_b)$ that satisfy the outage constraint constraint for the cellular network. Note that the other parameter p is determined by (q, λ_p). Assume that mobiles have large energy storage. For isotropic MPT, it is proved that

$$\mathcal{F}_h = \left\{(q, \lambda_p, \lambda_b) \in \mathbb{R}_+^3 \mid q\lambda_p\lambda_b^{\frac{\alpha}{2}} \geq c_2\right\}.$$

For directed MPT, an inner bound on $\mathcal{F}_h$ is obtained as:

$$\left\{(q, \lambda_p, \lambda_b) \in \mathbb{R}_+^3 \mid z_m q\lambda_p\lambda_b^{\frac{\alpha}{2}} \geq c_3\right\} \subset \mathcal{F}_h \quad (1)$$

where z_m denotes the array gain. The results quantify the tradeoffs between $(q, \lambda_p, \lambda_b)$ and show that the gain of MPT beamforming is equivalent to increasing q by a factor of z_m.

3) Assume that mobiles have small energy storage. To ensure stable transferred power, a constraint is applied such that the instantaneous received power at each mobile exceeds a given threshold with high probability. Under this and the outage constraint, inner bounds on $\mathcal{F}_h$ are obtained for isotropic MPT as

$$\left\{(q, \lambda_p, \lambda_b) \in \mathbb{R}_+^3 \mid q\lambda_p^{\frac{\beta}{2}}\lambda_b^{\frac{\alpha}{2}} \geq c_4, q\lambda_b^{\frac{\alpha}{2}} \geq c_5\right\} \subset \mathcal{F}_h \quad (2)$$

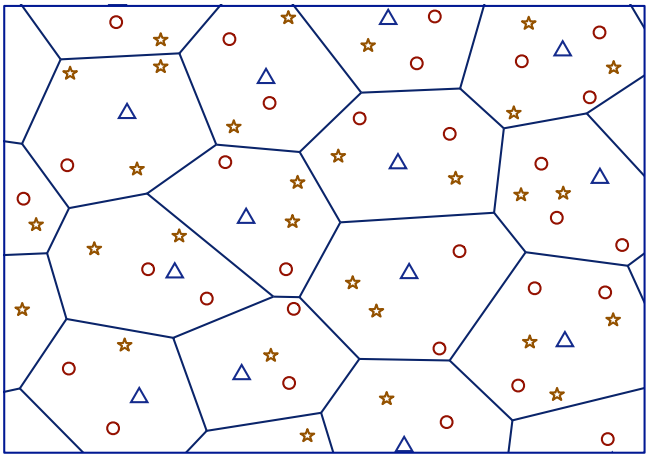

Fig. 2. Hybrid-network model where BSs, PBs and mobiles are marked with triangles, circles and stars, respectively. The Voronoi cells with respect to BSs are plotted with solid lines.

and for directed MPT as

$$\left\{(q, \lambda_p, \lambda_b) \in \mathbb{R}_+^3 \mid z_m q\lambda_p^{\frac{\beta}{2}}\lambda_b^{\frac{\alpha}{2}} \geq c_4, \; z_m q\lambda_b^{\frac{\alpha}{2}} \geq c_5\right\} \subset \mathcal{F}_h. \quad (3)$$

Similar remarks as on the result in (1) also apply to those in (2) and (3). Moreover, compared with their counterparts for mobiles with large energy storage, the current tradeoffs between λ_p and λ_b depend on the path-loss exponents for both data and MPT links. In particular, with other parameters fixed, λ_p decreases inversely with increasing λ_b if $\alpha = \beta$.

The remainder of the paper is organized as follows. The models, metrics and constraints are described in Section II. The feasibility regions for the cellular and hybrid networks are analyzed in Section III and IV, respectively. Numerical and simulation results are presented in Section V followed by concluding remarks in Section VI.

II. Models, Metrics and Constraints

A. Access-Network Model

BSs are modeled as a homogeneous PPP $\Phi = \{Y\}$ with density λ_b, where $Y \in \mathbb{R}^2$ represents the coordinates of the corresponding BS. Given that mobiles are associated with their nearest BSs, the horizontal plane is partitioned into Voronoi cells with points in Φ being the nuclei as illustrated in Fig. 2. It is assumed that the mobile density is much larger than the BS density such that there exists at least one active mobile in each cell almost surely. Mobiles in the same cell are i.i.d. and time share the corresponding BS. Time is divided into slots with unit durations. Each active mobile transmits a data packet with fixed power p in every slot. It is assumed that a mobile is scheduled with fixed probability denoted as ω and called the *duty cycle*. The scheduled mobile transmits data if it has sufficient energy. Note that a small duty cycle allows a mobile to harvest energy over a long duration for supporting bursty transmission. By applying Slyvnyak's Theorem [3], a *typical base station*, denoted as Y_0, is assumed to be located

at the origin without loss of generality. The active mobile served by Y_0 is called the *typical active mobile* and denoted as U_0. It is assumed that Y_0 uses a multiuser detector [27] to perfectly cancel interference from K nearest interfering mobiles. For ease of notation, let U_Y denote the active mobile served by BS Y and $\mathcal{C}$ represent the set of BSs serving K nearest interfering mobiles for Y_0. Channels are characterized by both path loss and small-scale fading such that signals transmitted by a mobile U with power a are received by BS Y with power $a\varphi G_{UY}|U-Y|^{-\alpha}$ where $\alpha > 2$ is the path-loss exponent, G_{UY} is a random variable modeling small-scale fading, and $|U-Y|$ is the Euclidian distance in meter between U and Y. The path-loss normalization factor φ is defined as $\varphi = s_0/d_0^{-\alpha}$ where d_0 is a reference distance in meter and s_0 is the propagation loss factor measured at d_0 [28]. A general distribution is assumed for $\{G_{UY}\}$ in the subsequent analysis. To simplify notation, let $G_{U_0Y_0}$ and G_{U_0Y} be re-denoted as G_0 and G_Y. Then it follows from the channel model that the signal power received at Y_0 is $p\varphi G_0|U_0|^{-\alpha}$ and the interference power is given as

$$I = p\varphi \sum_{Y\in\Phi\setminus\{Y_0,\mathcal{C}\}} G_Y|U_Y|^{-\alpha}. \tag{4}$$

The fading coefficients $\{G_Y \mid Y \in \Phi\}$ are assumed to be i.i.d. All channels are assumed fixed within one slot and independent over different slots. In addition, mobiles are assumed to have high mobility such that their random locations are independently distributed in different slots. Since the transmission and power transfer for each mobile are affected essentially by local BSs/PBs due to spatial separation, by the ergodicity of the BS/PB processes, the said assumption is equivalent to that a mobile experiences different realizations of the PB and BS processes in different slots, which overcomes some technicality in applying Lemma 2 in the sequel.

B. Power-Beacon Network Model

PBs are modeled as a homogeneous PPP, denoted as Ψ, with density λ_p and independent with the BS and mobile processes. Each mobile deploys a microwave-power receiver with a dedicated antenna as shown in Fig. 3 to intercept microwave energy transmitted by PBs. Inspired by the design in [29], the power receiver in Fig. 3 deploys two energy-storage units to enable continuous MPT. When a mobile is active, one unit is used for MPT and the other for powering the transmitter; their roles are switched when the latter unit is fully discharged. When the transmitter is inactive, the microwave-power receiver remains active till all units are fully recharged.

Consider isotropic MPT. A short-range propagation model [30] is used to avoid singularity caused by proximity between PBs and mobiles, thereby ensuring finite average power received by a mobile. To be specific, the instantaneous power received at the typical active mobile U_0 is given as

$$P = q\varphi' \sum_{T\in\Psi} [\max(|U_0 - T|, \nu)]^{-\beta} \tag{5}$$

where $\nu \geq 1$ is a constant, $\beta > 2$ is the path-loss exponent, and φ' is a path-loss normalization factor like φ and defined similarly as $\varphi' = s_0/d_0^{-\beta}$. Note that β need not be identical to the counterpart α for data links. Furthermore, the received signal power from other mobiles is neglected in (5) as it is much smaller than the received power due to PBs' transmission.

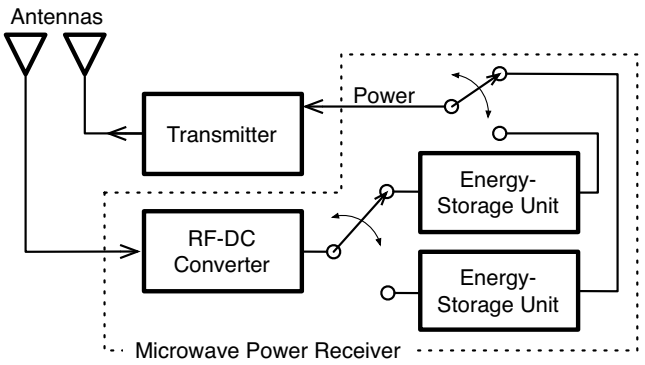

Fig. 3. A mobile consists of a transmitter and a microwave-power receiver. The latter uses two energy-storage units to enable simultaneous energy harvesting and powering a transmitter.

Next, consider directed MPT. Each mobile is constrained to be recharged by only the nearest PB using beamforming. To simplify analysis, the beamforming responses are assumed to have only two fixed levels, namely the main-lobe and side-lobe levels. A PB can serve multiple mobiles simultaneously where the total transmitted power is multiplied to ensure the reliability of MPT. Specifically, the transmission power of $T \in \Phi$ is $M_T q$ where M_T is the random number of mobiles for which T is the nearest PB. If the PBs are dense, some PBs may not be affiliated with any mobiles and are then turned off. Let the set of inactive PBs be denoted as Ψ_{off}. Note that all PBs are turned on in the case of isotropic MPT. Based on these assumptions and definitions, the instantaneous power received by U_0 can be written as

$$P = z_m q\varphi' \max\left(|U_0 - T_0|, \nu\right)^{-\beta} + z_s q\varphi' \sum_{T\in\Psi\setminus(\{T_0\}\cup\Psi_{\text{off}})} \max(|U_0 - T|, \nu)^{-\beta} \tag{6}$$

where the constants $z_m, z_s > 0$ represent the beam main-lobe and side-lobe responses, respectively. In contrast with the isotropic counterpart, directed MPT requires handshaking between PBs and mobiles e.g., using the following protocol. By estimating the relative distances and identifications of nearby PBs from their continuously broadcast signals, a mobile sends a recharging request and pilot symbols to the nearest PB that then estimate the mobile direction and beam's power in this direction.

C. Metrics and Constraints

The cellular-network performance is measured by the outage probability that also gives the fraction of mobiles outside network coverage [22]. Define the outage probability for the typical BS Y_0 as

$$P_{\text{out}} = \Pr\left(\frac{p\varphi G_0|U_0|^{-\alpha}}{I+\sigma^2} < \theta\right)$$

where I is given in (4), σ^2 is positive and denotes the channel-noise variance, and θ is the target SINR.

Constraint 1 (Cellular network)**.** The cellular-network deployment satisfies the *outage constraint* at BSs: $P_{\mathsf{out}} \leq \epsilon$ with $0 < \epsilon < 1$.

Mobiles store energy in either large storage unites (e.g., rechargeable batteries) or small ones (e.g., super capacitors). Large storage at a mobile removes the randomness of instantaneous received power and provides fixed output power (see Lemma 2). However, given small storage, the transmission power of a mobile may fluctuate due to the random locations of PBs. The fluctuation is suppressed by ensuring sufficiently large and stable *instantaneous* power transferred to each mobile. Define a *power outage* as an event that the instantaneous received power at each mobile is below the mobile transmission power p and the probability for such an event is called the *power-outage probability*.

Constraint 2 (Power beacons)**.** The PB deployment satisfies the following constraints. For the case of large energy storage, the power-outage probability is zero. For the case of small energy storage, the power-outage probability should be no larger than a constant δ with $0 < \delta < 1$, called the *power-outage constraint*.

The probability δ is chosen to be sufficiently small such that a power outage at an active mobile can be coped with by drawing energy buffered in the small storage units to ensure uninterrupted transmission with power p.

III. Access-Network Deployment

In this section, the requirements for the cellular-network parameters (p, λ_b) are investigated by deriving the feasibility region $\mathcal{F}_c$. It is found that $\mathcal{F}_c$ for the case of interference-limited networks is independent with the outage constraint.

A. Access-Network Deployment with Nonzero Noise

To characterize the feasibility region, a useful result is obtained as shown in Lemma 1 that is proved in Appendix A using Mapping Theorem [31].

Lemma 1. Consider the BS process Φ as a function of the density λ_b denoted as $\Phi(\lambda_b)$. The two random variables $\sum_{Y\in\Phi(\lambda_b)} h_Y |U_Y|^{-\alpha}$ and $\sum_{Y\in\Phi(a\lambda_b)} a^{-\frac{\alpha}{2}} h_Y |U_Y|^{-\alpha}$ follow an identical distribution, where $a > 0$ and $h_Y \in \mathbb{R}$ depends only on Y.

Furthermore, define $\mu > 0$ as a constant for given ϵ and a stationary distribution of $\{G_Y\}$ such that

$$\Pr\left(\sum_{Y\in\Phi(1)} \left[G_Y|U_Y|^{-\alpha}1\{Y \neq Y_0 \cup \mathcal{C}\} - \theta^{-1}G_0|U_0|^{-\alpha}1\{Y = Y_0\}\right] + \mu > 0\right) = \epsilon. \tag{7}$$

The main result of this section is shown in the following proposition.

Proposition 1. Assume that the outage probability is strictly smaller than ϵ in the absence of noise ($\sigma^2 = 0$). Under Constraint 1, the feasibility region for the cellular network with nonzero noise is

$$\mathcal{F}_c = \left\{(\lambda_b, p) \in \mathbb{R}_+^2 \mid p\lambda_b^{\frac{\alpha}{2}} \geq \frac{\sigma^2}{\varphi\mu}\right\} \tag{8}$$

with μ defined in (7) and $\sigma^2 > 0$.

Proof: First of all, the assumption in the proposition statement ensures that μ in (7) is strictly positive. Consider the outage probability $P_{\mathsf{out}}(\cdot,\cdot)$ as a function of (λ_b, p). To facilitate analysis, the outage probability can be rewritten as

$$P_{\mathsf{out}}(\lambda_b, p) = \Pr\left(\sum_{Y\in\Phi(\lambda_b)} \left[G_Y|U_Y|^{-\alpha}1\{Y \neq Y_0 \cup \mathcal{C}\} - \theta^{-1}G_0|U_0|^{-\alpha}1\{Y = Y_0\}\right] + \frac{\sigma^2}{p\varphi} > 0\right). \tag{9}$$

Using (9) and Lemma 1, it can be obtained that

$$P_{\mathsf{out}}(\lambda_b, p) = \Pr\left(\sum_{Y\in\Phi(1)} \left[G_Y|U_Y|^{-\alpha}1\{Y \neq Y_0 \cup \mathcal{C}\} - \theta^{-1}G_0|U_0|^{-\alpha}1\{Y = Y_0\}\right] + \frac{\sigma^2}{p\varphi\lambda_b^{\frac{\alpha}{2}}} > 0\right). \tag{10}$$

Since the summation in (10) is a continuous random variable, $P_{\mathsf{out}}(p, \lambda_b) \leq \epsilon$ for all $\sigma^2/(p\varphi\lambda_b^{\alpha}) \leq \mu$. The desired result follows. ∎

Remark 1. The result in Proposition 1 is consistent with the intuition that deploying denser BSs shortens transmission distances and hence requires lower transmission power at mobiles. In particular, doubling λ_b decreases p by a factor of $2^{\frac{\alpha}{2}}$, which is more significant for more severe propagation attention (larger α).

Remark 2. It is challenging to derive a closed-form expression for μ defined in (7) and its relation with ϵ is evaluated via simulation in the sequel. However, some simple properties of the relation can be inferred as follows: a) $\epsilon(\mu)$ is a strictly monotone increasing function of μ, b) $\epsilon(0)$ corresponds to interference limited networks and c) $\lim_{\mu\to\infty} \epsilon(\mu) = 1$.

B. Access-Network Deployment with Zero Noise

Consider an interference-limited cellular network where noise is negligible.

Proposition 2. For an interference-limited cellular network with zero noise, P_{out} is independent with the BS density λ_b and mobile-transmission power p.

Proof: By substituting $\sigma^2 = 0$ into (9), the outage probability can be written as

$$P_{\mathsf{out}} = \Pr\left(\sum_{Y\in\Phi} \left[G_Y|U_Y|^{-\alpha}1\{Y \neq Y_0 \cup \mathcal{C}\} - \theta^{-1}G_0|U_0|^{-\alpha}1\{Y = Y_0\}\right] > 0\right). \tag{11}$$

Let P_{out} and the BS process Φ be functions of λ_b, denoted as $P_{\mathsf{out}}(\lambda_b)$ and $\Phi(\lambda_b)$, respectively. Using (11) and given $a>0$, $P_{\mathsf{out}}(a\lambda_b)$ can be written as

$$P_{\mathsf{out}}(a\lambda_b) = \Pr\left(\sum_{Y\in\Phi(a\lambda_b)} \left[G_Y|U_Y|^{-\alpha}1\{Y\neq Y_0\cup\mathcal{C}\}- \theta^{-1}G_0|U_0|^{-\alpha}1\{Y=Y_0\}\right]>0\right)$$

$$= \Pr\left(\sum_{Y\in\Phi(\lambda_b)} \left[G_Y|U_Y|^{-\alpha}1\{Y\neq Y_0\cup\mathcal{C}\}- \theta^{-1}G_0|U_0|^{-\alpha}1\{Y=Y_0\}\right]>0\right) \quad (12)$$

$$= P_{\mathsf{out}}(\lambda_b) \quad (13)$$

where (12) applies Lemma 1 and (13) follows from (11). The proposition statement is a direct result of (13), completing the proof. ∎

Remark 3. The dual of the result in Proposition 2 for downlink networks without interference cancelation is shown in [22] using the method of Laplace transform. These results are the consequence of the fact that in both uplink and downlink interference-limited networks, transmission power has no effect on the *signal-to-interference ratio* (SIR), and increasing the BS density shortens the distances of data and interference links by the same factor and hence also has no effect on the SIR.

Remark 4. For interference-limited networks, the outage probability is determined by the number of antennas used at each BS for interference cancellation as well as the outage threshold θ and the pass-loss exponent α that determines the level of spatial separation.

Remark 5. Though outage probability is independent with λ_b in an interference-limited network, the network throughput grows linearly with increasing λ_b since denser active mobiles can be supported.

Remark 6. One should not interpret the result in Proposition 2 as that the BS density and mobile transmission power can be arbitrarily small without affecting the outage probability. In contrast, the said density and power have to be sufficiently large to ensure the dominance of the interference over noise that is the condition for the proposition to hold.

IV. Hybrid-Network Deployment

In this section, the hybrid-network deployment is analyzed by deriving the feasibility region $\mathcal{F}_h$ for different PB-network configurations combining isotropic/directed MPT and large/small energy storage at mobiles.

A. Hybrid-Network Deployment: Mobiles with Large Energy Storage

In this section, it is assumed that energy-storage units (see Fig. 3) at mobiles have infinite capacity. Large storage provides active mobiles reliable transmission power as specified in the following lemma directly following from [25, Theorem 1] that studies energy harvesting in MANETs.

Lemma 2 ([25])**.** For mobiles with infinite energy storage and powered by MPT, the probability that a mobile can transmit signals with power p is given as

$$\Pr(P\geq p) = \begin{cases} 1, & \mathsf{E}[P]\geq \omega p \\ \dfrac{\mathsf{E}[P]}{\omega p}, & \text{otherwise} \end{cases} \quad (14)$$

where P is the instantaneous received power in (5) and (6) for isotropic and directed MPT, respectively.

Lemma 2 suggests that an active mobile can transmit signals continuously with power up to $\mathsf{E}[P]/\omega$. Closed-form expressions for $\mathsf{E}[P]$ are derived by applying Campbell's Theorem [31]. The results are shown in Lemma 3.

Lemma 3. The average received power for a mobile due to PBs' transmission is given as follows:

1) for isotropic MPT,

$$\mathsf{E}[P] = \frac{\pi\beta\nu^{2-\beta}q\varphi'\lambda_p}{\beta-2}; \quad (15)$$

2) for directed MPT,

$$\mathsf{E}[P] \geq z_m q\varphi'\left[\nu^{-\beta}\left(1-e^{-\pi\lambda_p\nu^2}\right)+ (\pi\lambda_p)^{\frac{\beta}{2}}\gamma\left(\pi\lambda_p\nu^2, 1-\frac{\beta}{2}\right)\right]. \quad (16)$$

The proof of Lemma 3 is provided in Appendix B.

Remark 7. One can observe from Lemma 3 that the expected received power for the case of isotropic MPT is infinite for β equal to two. The reason is that β being too small corresponds to low propagation loss such that even the transmission of a far-away PB leads to significant received power at a mobile; the influence of a large number of PBs causes the total received power to diverge. The extreme case of β being two does not hold in practice except for very short transfer distances and the typical value for β falls in the range of three to five.

Remark 8. For isotropic MPT, a mobile is powered by all nearby PBs and thus the expected received power $\mathsf{E}[P]$ given in (15) is proportional to the PB density λ_p. $\mathsf{E}[P]$ is also proportional to the PB-transmission power q.

Remark 9. For directed MPT, if $\lambda_p\nu^2 \ll 1$, hence $\mathsf{E}[P]\approx \pi z_m q\lambda_p\varphi'\nu^{2-\beta}$ that is equal to the counterpart for isotropic MPT in (15) with the factor $\frac{\beta}{\beta-2}$ replaced with z_m. It is important to note that these two factors represent respectively the advantages of isotropic and directed MPT, namely that strong power received by a mobile results form a large number of PBs for the case of isotropic MPT with low propagation loss (β is close to 2) and from sharp beamforming for the case of directed MPT (large z_m).

The main result of this section is shown in Proposition 3, which follows from combining Constraint 2, Proposition 1 and Lemma 2 and 3.

Proposition 3. Given mobiles with infinite energy storage, the feasibility region $\mathcal{F}_h$ for the hybrid network deployed under the outage constraint is as follows.

1) For isotropic MPT,

$$\mathcal{F}_h = \left\{(q,\lambda_b,\lambda_p) \in \mathbb{R}_+^3 \mid q\lambda_p\lambda_b^{\frac{\alpha}{2}} \geq \left(1-\frac{2}{\beta}\right)\frac{\omega\sigma^2\nu^{\beta-2}}{\pi\varphi\varphi'\mu}\right\}. \tag{17}$$

2) For directed MPT, $\mathcal{F}_n$ is inner bounded as

$$\left\{(q,\lambda_b,\lambda_p) \in \mathbb{R}_+^3 \mid z_m q\lambda_b^{\frac{\alpha}{2}}\left(1-e^{-\pi\lambda_p\nu^2}\right) \geq \frac{\omega\sigma^2\nu^{\beta}}{\varphi\varphi'\mu}\right\} \subset \mathcal{F}_h. \tag{18}$$

The inner bound on $\mathcal{F}_h$ as given in (18) results from the following inequality from Lemma 3:

$$\mathsf{E}[P] \geq z_m q\varphi'\nu^{-\beta}\left(1-e^{-\pi\lambda_p\nu^2}\right)$$

combined with Proposition 1 and Lemma 2.

Remark 10. For isotropic MPT, the required PB density decreases with the increasing PB transmission power q and BS density λ_b as shown in (17). The result also shows the effects of the path-loss exponents α and β for data and MPT links, respectively. Specifically, the required PB density diminishes as β approaches 2 corresponding to fee-space propagation and increases with growing α for which data-link path loss is more severe and higher transmission power at mobiles is needed. In addition, for both isotropic and directed MPT, the required PB density is proportional to the mobile duty cycle ω.

If the exponent $\pi\lambda_p\nu^2$ is small, the inner bound on $\mathcal{F}_h$ can be simplified as shown in the following corollary.

Corollary 1. Given mobiles with infinite energy storage and powered by directed MPT, as $\lambda_p\nu^2 \to 0$, the feasibility region $\mathcal{F}_h$ for the hybrid network deployed under the outage constraint can be inner bounded as

$$\left\{(q,\lambda_b,\lambda_p) \in \mathbb{R}_+^3 \mid z_m q\lambda_p\lambda_b^{\frac{\alpha}{2}} \geq \frac{\omega\sigma^2\nu^{\beta-2}}{\pi\varphi\varphi'\mu} + o(1)\right\} \subset \mathcal{F}_h.$$

It is observed that the inner bound on the feasibility region in the corollary has a similar form as the feasibility region in (17) for isotropic MPT where z_m represents the amplification of transferred power by beamforming.

B. Hybrid-Network Deployment: Mobiles with Small Energy Storage

For the current case, the deployment of the hybrid network has to satisfy both Constraints 1 and 2. The derivation of the resultant feasibility region requires analyzing the cumulative-distribution function (CDF) of the instantaneous received power at a mobile that is a summation over a PPP. Though the function has no closed form [32], it can be upper bounded as shown in the following lemma by considering only the nearest PB for a mobile.

Lemma 4. Given mobiles with small energy storage, the power-outage probability is upper bounded as follows:

1) for isotropic MPT, if $q\varphi'\nu^{-\beta} \geq p$,

$$\Pr(P<p) \leq e^{-\pi\lambda_p\left(q\varphi'/p\right)^{\frac{2}{\beta}}}; \tag{19}$$

2) for directional MPT, if $z_m q\varphi'\nu^{-\beta} \geq p$,

$$\Pr(P<p) \leq e^{-\pi\lambda_p\left(z_m q\varphi'/p\right)^{\frac{2}{\beta}}}. \tag{20}$$

The proof of Lemma 4 is provided in Appendix C. The conditions in Lemma 4, namely $q\nu^{-\beta} \geq p$ for isotropic MPT and $z_m q\nu^{-\beta} \geq p$ for directed MPT, ensure that a PB can deliver sufficient power to a mobile when they are sufficiently near.

Remark 11. The bound on the power-outage probability is tight only for the case of directed MPT where the nearest PB for a mobile is the dominant power source due to beamforming. For isotropic MPT, a mobile may receive comparable powers from multiple nearby PBs and considering only one of them is insufficient to give a tight bound. Deriving such a bound requires quantifying the distribution of the total received power which is a shot-noise process and known to have no simple form. The remark on the tightness of the bounds also applies to that of the resultant inner bounds on the feasibility regions as confirmed by simulation results in the sequel.

Combining the results in Proposition 1, Lemma 4 and applying Constraint 3 give the main result of this section as shown below.

Proposition 4. Given mobiles with small energy storage, the feasibility region $\mathcal{F}_h$ for the hybrid network deployed under Constraint 1 and 3 can be inner bounded as follows:

1) for isotropic MPT,

$$\left\{(q,\lambda_b,\lambda_p) \in \mathbb{R}_+^3 \mid q\lambda_p^{\frac{\beta}{2}}\lambda_b^{\frac{\alpha}{2}} \geq \left(\frac{\log\frac{1}{\delta}}{\pi}\right)^{\frac{\beta}{2}}\frac{\sigma^2}{\varphi'\varphi\mu}, q\lambda_b^{\frac{\alpha}{2}} \geq \frac{\sigma^2\nu^{\beta}}{\varphi\varphi'\mu}\right\} \subset \mathcal{F}_h;$$

2) for directional MPT,

$$\left\{(q,\lambda_b,\lambda_p) \in \mathbb{R}_+^3 \mid z_m q\lambda_p^{\frac{\beta}{2}}\lambda_b^{\frac{\alpha}{2}} \geq \left(\frac{\log\frac{1}{\delta}}{\pi}\right)^{\frac{\beta}{2}}\frac{\sigma^2}{\varphi'\varphi\mu}, z_m q\lambda_b^{\frac{\alpha}{2}} \geq \frac{\sigma^2\nu^{\beta}}{\varphi\varphi'\mu}\right\} \subset \mathcal{F}_h.$$

It can be observed from the results that the product of the PB parameters, namely $q\lambda_p^{\frac{\beta}{2}}$, is proportional to the logarithm of the maximum power-shortage probability δ and hence insensitive to changes on δ. Moreover, the results in Proposition 4 show that beamforming reduces the required $q\lambda_p^{\frac{\beta}{2}}$ by the factor of z_m. Like the case of mobiles having large energy storage, the required value of $q\lambda_p^{\frac{\beta}{2}}$ for the current case also decreases with increasing BS density but at a different rate.

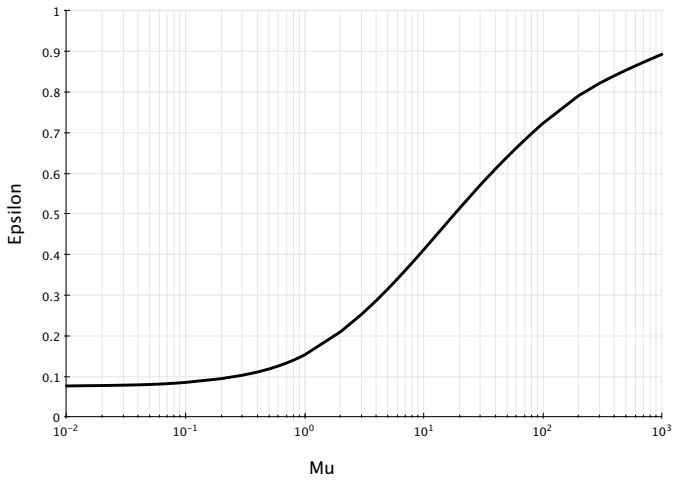

Fig. 4. ϵ versus μ defined in (7).

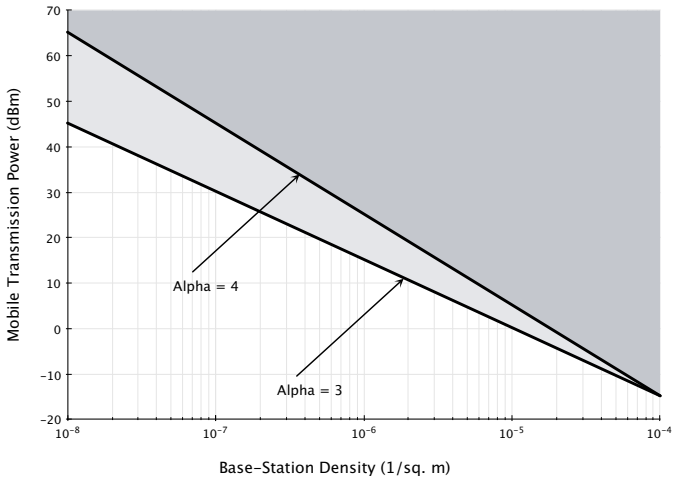

Fig. 5. Feasibility region for the cellular network for the path-loss exponent $\alpha = \{3, 4\}$.

V. Numerical and Simulation Results

The results in the section are obtained based on the following values of parameters unless specified otherwise. The path-loss exponents are $\alpha = 4$ and $\beta = 3$ and the outage threshold is $\theta = 1$. The path-loss normalization factors φ and φ' are computed based on the reference distance $d_0 = 100$ meters and the pass-loss $s_0 = 70$ dB measured at d_0, which are typical values for a microcellular network [28]. For the MPT path loss model, $\nu = 1$. The channel fading coefficients are i.i.d. and follow the same distribution as $|G|^2$ where G is a symmetric $\mathcal{CN}(1, 0.1)$ random variable, modeling Rician fading. Each BS cancels interference from $K = 5$ nearest unintended mobiles. The maximum outage probability in Constraint 1 is $\epsilon = 0.1$ and the maximum power-outage probability is $\delta = 0.1$. For directional MPT, the beam main-lobe and side-lobe responses are $z_m = 10$ and $z_s = 0.2$. Last, the PB transmission power and the noise variance are fixed as $q = 20$ W and $\sigma^2 = -90$ dBm.

A. Access-Network Deployment

The curve of ϵ versus μ defined in (7) is plotted in Fig. 4 and observed to be consistent with Remark 2 on Proposition 1. In particular, ϵ approaches 1 as μ increases and its minimum value (0.096) at $\mu = 0$ gives the outage probability for an interference-limited network. In addition, it is observed that $\mu = 0.3$ corresponds to $\epsilon = 0.1$ used in simulation.

The feasibility region $\mathcal{F}_c$ for the cellular network as given in Proposition 1 is plotted in Fig. 5 for $\alpha = \{3, 4\}$. It is observed that increasing α (more severe path loss) leads to larger mobile transmission power q given fixed BS density λ_b and outage probability, shrinking the feasibility region. The effect diminishes as the BS density grows. In addition, the minimum p in dBm is observed to decrease linearly with increasing $\log \lambda_b$.

B. Hybrid-Network Deployment

Fig. 6 shows the curves of mobile-transmission power p versus BS density λ_p for different combinations between large/small energy storage at mobiles and isotropic/directional MPT. The curves for the case of large energy storage are computed numerically using Lemma 3 and those for the case of small storage are obtained by simulation. It is observed that deploying large energy storage units at mobiles can dramatically increase p when λ_p is small e.g., the gain is more than 35 dB for $\lambda_p = 10^{-5}$ and directed MPT. Such gain diminishes as λ_p (or equivalently the MPT efficiency) increases. Next, beamforming (directed MPT) supports larger p than isotropic MPT especially for the case of large storage. Last, the values of p for directional MPT are insensitive to changes on λ_p if it is sufficiently large. The reason is that p is dominated by the maximum power transferred to a mobile from the nearest PB that approaches a constant $q\nu^{-\alpha}$. In contrast, the value of p (in dB) for isotropic MPT does not saturate and increases approximately logarithmically with growing λ_p.

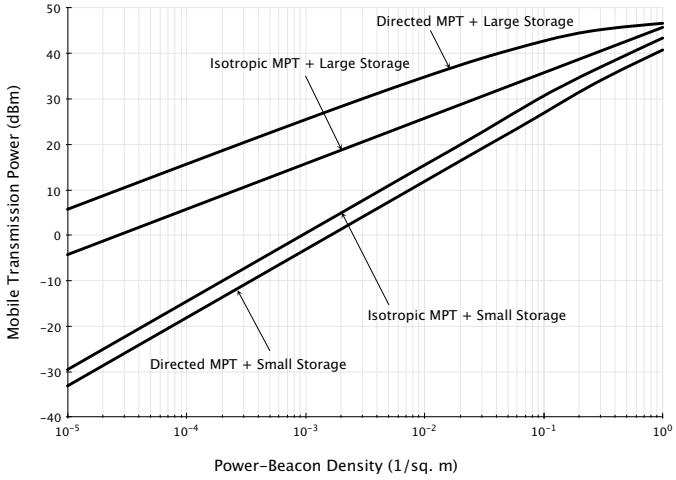

Fig. 6. Mobile-transmission power versus PB density for different combinations between large/small energy storage at mobiles and isotropic/directional MPT.

In Fig. 7, the feasibility regions for the hybrid network are plotted for different cases accounting for large/small

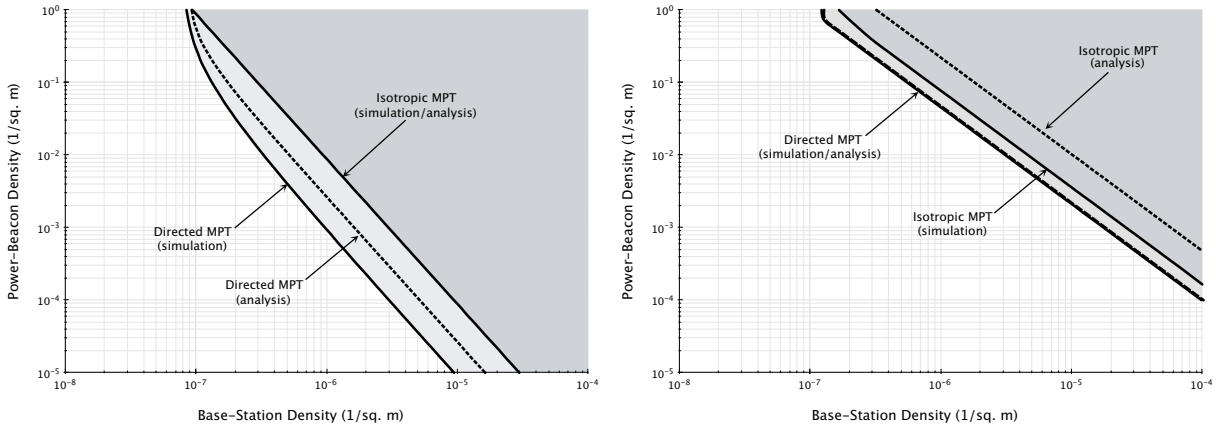

Fig. 7. Feasibility regions (shaded areas) for the hybrid network: (left) mobiles with large storage and (right) mobiles with small storage. The boundaries of the inner bounds on the feasibility regions are plotted with dashed lines.

energy storage at mobiles and isotropic/directional MPT. The feasibility region for the case of isotropic MPT with large energy storage is obtained using Proposition 1 and those for other cases by simulation. First of all, direct MPT is observed to achieve larger feasibility regions than isotropic MPT in the considered practical ranges of λ_p and λ_b. Next, also shown in the figures are inner bounds on the feasibility regions based on Proposition 3 and 4 with their boundaries plotted with dashed lines. The bound for the case of directed MPT with small energy storage is observed to be tight due to the presence of a dominant PB for each mobile, which matches the assumption made in the derivation of the bound. Last, by inspecting the feasibility regions for directed MPT, there exists a threshold on the BS density below which the required PB density grows extremely rapidly. The BS density above the threshold corresponds to the regime where the power transferred to a mobile from the nearest PB is larger than the minimum required for satisfying the outage constraint on the cellular network. Otherwise, besides receiving power from the nearest PB, mobiles rely on accumulating power from unintended PBs via their side-lobe transmissions so as to satisfy the outage constraint, resulting in a high required PB density. The said threshold on the BS density, denoted as λ_b^*, can be obtained from Proposition 3 and 4 as

$$\lambda_b^* = \begin{cases} \left(\dfrac{\omega\sigma^2\nu^\beta}{z_m q\varphi\varphi'\mu}\right)^{\frac{2}{\alpha}}, & \text{large energy storage} \\ \left(\dfrac{\sigma^2\nu^\beta}{z_m q\varphi\varphi'\mu}\right)^{\frac{2}{\alpha}}, & \text{small energy storage} \end{cases} \tag{21}$$

which specifies the left boundaries of the inner bounds on the feasibility regions for the case of directed MPT (see Fig. 7).

VI. Concluding Remarks

The deployment of PBs for powering a cellular network via MPT has been investigated based on a stochastic-geometry network model, resulting in simple tradeoffs between network parameters. First, considering the cellular network under an outage constraint, the minimum mobile-transmission power p has been shown to increase super-linearly with the decreasing base-station density λ_b. However, the absence of noise renders outage probability independent with (p, λ_b). Next, building on these results, the requirements on the PB deployment have been studied by analyzing the tradeoff between λ_b and the PB transmission power q and density λ_p. Given isotropic MPT and mobiles having large capacity for storing transferred energy, the product $q\lambda_p\lambda_b^{\frac{\alpha}{2}}$ is required to be above a given threshold so as to satisfy the outage constraint. For the case of mobiles having small energy storage, both the products $q\lambda_p^{\frac{\beta}{2}}\lambda_b^{\frac{\alpha}{2}}$ and $q\lambda_b^{\frac{\alpha}{2}}$ should be sufficient large. It has been found that compared with isotropic MPT, directed MPT by beamforming effectively increases q by the array gain.

This work relies on a stochastic-geometry network model and various simplifying assumptions to derive tradeoffs between network parameters. The results provide first-order guidelines for realizing MPT in cellular networks. To derive more elaborate insight into MPT implementation, further investigations in practical settings are necessary by considering the dependance of the directed-MPT efficiency on the array configurations, using realistic channel models for small-cell networks, modeling the hotspot deployment of PBs using a clustered point process, characterizing the effect of mobility on MPT, and taking into account the dynamics of energy-levels at mobiles.

Appendix

A. Proof of Lemma 1

To facilitate the proof, re-denote $\{(U_Y, h_Y) \mid Y \in \Phi\}$ as $\{(U_n, h_n)\}_{n=1}^{\infty}$. It is almost surely that given Φ and an arbitrary active mobile U_n, there exists a set of coefficients $\{c_{n,Y} \mid Y \in \Phi\}$ such that $U_n = \sum_{Y\in\Phi} c_{n,Y} Y$. Consequently, a set of random coefficients $\{C_{n,Y} \mid Y \in \Phi\}$ can be defined under the constraint that $U_n = \sum_{Y\in\Phi} C_{n,Y} Y$ is uniformly distributed in the corresponding Voronoi cell. It follows that

$$\sum_{Y\in\Phi(\lambda_b)} h_Y |U_Y|^{-\alpha} = \sum_{n=1}^{\infty} h_n \left| \sum_{Y\in\Phi(\lambda_b)} C_{n,Y} Y \right|^{-\alpha}. \tag{22}$$

Given $a > 0$ and $\Phi(\lambda_b)$, define a function $f : \mathbb{R}^2 \to \mathbb{R}^2$ such that for $\mathcal{A} \subset \mathbb{R}^2$, $f(\mathcal{A}) = \{\sqrt{a}x \mid x \in \mathcal{A}\}$. Intuitively,

f expands (or shrink) the Euclidean plane by a factor a if $a > 1$ (or $a < 1$). Let η denote the mean measure of $\Phi(a\lambda_b)$ and define a measure $\eta^*(\mathcal{B})$ with $\mathcal{B} \subset \mathbb{R}^2$ as $\eta^*(\mathcal{B}) = \eta(f^{-1}(\mathcal{B}))$. It follows that $\eta^*(\mathcal{B}) = \lambda_b|\mathcal{B}|$ where $|\mathcal{B}|$ denotes the measure (area) of $\mathcal{B}$. Since f is a measurable function that does not map distinct points to a single point, applying Mapping Theorem [31, p18] gives that $f(\Phi(a\lambda_b))$ is a homogeneous PPP with density λ_b. As a result, the random variable $\sum_{Y\in\Phi(a\lambda_b)} C_{n,Y} f(Y)$ is identically distributed as $\sum_{Y\in\Phi(\lambda_b)} C_{n,Y} Y$. Combining this fact and (22) yields the desired result. ■

B. Proof of Lemma 3

For isotropic MPT, using (5) and applying Campbell's Theorem give

$$\begin{aligned}\mathsf{E}[P] &= q\varphi'\lambda_p \int_{x\in\mathbb{R}^2} [\max(|x-U_0|,\nu)]^{-\beta}\, dx \\ &= 2q\varphi'\pi\lambda_p \int_0^\infty [\max(r,\nu)]^{-\beta}\, r dr \qquad (23)\\ &= 2q\varphi'\pi\lambda_p\nu^{-\beta}\int_0^\nu r dr + 2q\varphi'\pi\lambda_p\int_\nu^\infty r^{1-\beta} dr \qquad (24)\end{aligned}$$

where (23) results from the stationarity of Ψ and using the polar-coordinate system. The corresponding expression of $\mathsf{E}[P]$ in (15) follows from (24).

Next, consider directed MPT and the corresponding expression for $\mathsf{E}[P]$ is derived as follows. Using (6) and omitting the side-lobe contributions from unintended PBs, P is lower bounded as

$$P \geq z_m q\varphi' \max\left(|U_0 - T_0|, \nu\right)^{-\beta}. \qquad (25)$$

For ease of notation, define $D = |U_0 - T_0|$. It follows that

$$\mathsf{E}[P] \geq z_m q\varphi' \mathsf{E}\left[\max(D,\nu)^{-\beta}\right]. \qquad (26)$$

Note that D measures the shortest distance between a point in the PPP Ψ to a fixed point and have the following probability-density function [33]

$$f_D(r) = 2\pi\lambda_p r e^{-\pi\lambda_p r^2}, \qquad r \geq 0. \qquad (27)$$

Given the distribution, it is obtained that

$$\begin{aligned}\mathsf{E}\left[\max(D,\nu)^{-\beta}\right] &= 2\pi\lambda_p\int_0^\infty \max(r,\nu)^{-\beta} r e^{-\pi\lambda_p r^2} dr \\ &= 2\pi\lambda_p\int_0^\nu \nu^{-\beta} r e^{-\pi\lambda_p r^2} dr + \\ &\qquad 2\pi\lambda_p\int_\nu^\infty r^{1-\beta} e^{-\pi\lambda_p r^2} dr \\ &= \nu^{-\beta}\left(1 - e^{-\pi\lambda_p\nu^2}\right) + \\ &\qquad (\pi\lambda_p)^{\frac{\beta}{2}}\gamma\left(\pi\lambda_p\nu^2, 1-\frac{\beta}{2}\right). \qquad (28)\end{aligned}$$

Substituting (28) into (26) gives the desired result in (16), completing the proof. ■

C. Proof of Lemma 4

Without loss of generality, assume that U_0 is located at the origin o since according to Slyvnyak's Theorem,

$$\Pr(P < p) = \Pr(P < p \mid U_0 = o) \qquad (29)$$

where P is given in (5) and (6) for isotropic and directed MPT, respectively. The previous assumption that Y_0 is at the origin is unnecessary for the proof.

Consider isotropic MPT. Define $r_0 = (q\varphi'/p)^{\frac{1}{\beta}}$. Note that any PB with a distance r_0 from U_0 can supply received raw power higher than p. Furthermore, $r_0 \geq \nu$ as a result of the assumption $q\varphi'\nu^{-\beta} \geq p$. Inspired by the approach in [34] that studies outage probability for mobile ad hoc networks, the probability of no power shortage is expanded as

$$\begin{aligned}&\Pr(P \geq p) = \Pr(\Phi \cap B(0,r_0) \neq \emptyset) + \\ &\Pr(P \geq p \mid \Phi \cap B(0,r_0) = \emptyset)\Pr(\Phi \cap B(0,r_0) = \emptyset)\end{aligned} \qquad (30)$$

where $B(a,b)$ is a disk centered at $a \in \mathbb{R}^2$ and with a radius $b \geq 0$. It follows that the power-shortage probability can be lower bounded as

$$\begin{aligned}\Pr(P \geq p) &\geq \Pr(\Phi \cap B(0,r_0) \neq \emptyset) \\ &= 1 - e^{-\pi\lambda_p r_0^2}. \qquad (31)\end{aligned}$$

The derived result in $1)$ in the lemma statement follows.

The result for directed MPT can be obtained similarly. This completes the proof. ■

REFERENCES

[1] T. L. Marzetta, "Noncooperative cellular wireless with unlimited numbers of base station antennas," *IEEE Trans. Wireless Commun.*, vol. 9, pp. 3590–3600, Sept. 2010.

[2] V. Chandrasekhar, J. G. Andrews, and A. Gatherer, "Femtocell networks: a survey," *IEEE Commun. Mag.*, vol. 46, pp. 59–67, Sept. 2008.

[3] D. Stoyan, W. S. Kendall, and J. Mecke, *Stochastic Gemoetry and its Applications*, 2nd ed. Wiley, 1995.

[4] R. Want, "An introduction to RFID technology," *IEEE Pervasive Comput.*, vol. 5, pp. 25–33, Jan. 2006.

[5] A. Kurs, A. Karalis, R. Moffatt, J. D. Joannopoulos, P. Fisher, and M. Soljačić, "Wireless power transfer via strongly coupled magnetic resonances," *Science*, vol. 317, pp. 83–86, July 2007.

[6] W. C. Brown, "The history of power transmission by radio waves," *IEEE Trans. Microwave Theory Techniques*, vol. 32, pp. 1230–1242, Sept. 1984.

[7] W. C. Brown, "Experiments involving a microwave beam to power and position a helicopter," *IEEE Trans. Aerospace Electron. Syst.*, vol. AES-5, pp. 692–702, Sept. 1969.

[8] J. J. Schlesak, A. Alden, and T. Ohno, "A microwave powered high altitude platform," *IEEE MTT-S Digest*, pp. 283–286, 1988.

[9] H. Matsumoto, "Research on solar power satellites and microwave power transmission in Japan," *IEEE Microwave Mag.*, vol. 3, pp. 36–45, Dec. 2002.

[10] J. O. Mcspadden and J. C. Mankins, "Space solar power programs and microwave wireless power transmission technology," *IEEE Microwave Mag.*, vol. 3, pp. 46–57, Apr. 2002.

[11] L. R. Varshney, "Transporting information and energy simultaneously," in *Proc. 2008 IEEE Intl. Symp. Inf. Theory*, pp. 1612–1616.

[12] P. Grover and A. Sahai, "Shannon meets Tesla: wireless information and power transfer," in *Proc. 2010 IEEE Intl. Symp. Inf. Theory*, pp. 2363–2367.

[13] X. Zhou, R. Zhang, and C.-K. Ho, "Wireless information and power transfer: architecture design and rate-energy tradeoff," *IEEE Trans. Commun.*, vol. 61, pp. 4754–4767, Nov. 2013.

[14] R. Zhang and C. Ho, "MIMO broadcasting for simultaneous wireless information and power transfer," *IEEE Trans. Wireless Commun.*, vol. 12, pp. 1989–2001, May 2013.

[15] Z. Xiang and M. Tao, "Robust beamforming for wireless information and power transmission," *IEEE Wireless Commun. Lett.*, vol. 1, pp. 372–375, Apr. 2012.
[16] P. Popovski, A. Fouladgar, and O. Simeone, "Interactive joint transfer of energy and information," *IEEE Trans. Commun.* vol. 61, no. 5, pp. 2086–2097, May 2013.
[17] B. Gurakan, O. Ozel, J. Yang, and S. Ulukus, "Energy cooperation in energy harvesting wireless communications," in *Proc. 2012 IEEE Intl. Symp. Inf. Theory*, pp. 965–969.
[18] K. Huang and E. G. Larsson, "Simultaneous information-and-power transfer for broadband downlink systems," *IEEE Trans. Signal Process.*, vol. 61, pp. 5972–5986, Dec. 2013.
[19] D. W. Ng, E. S. Lo, and R. Schober, "Energy-efficient resource allocation in multiuser OFDM systems with wireless information and power transfer," in *Proc. 2013 IEEE Wireless Commun. Netw. Conf.*, pp. 3823–3828.
[20] S. G. Foss and S. A. Zuyev, "On a Voronoi aggregative process related to a bivariate Poisson process," *Advances Applied Prob.*, vol. 28, pp. 965–981, Dec. 1996.
[21] F. Baccelli, M. Klein, M. Lebourges, and S. Zuyev, "Stochastic geometry and architecture of communication networks," *Telecomm. Syst.*, vol. 7, no. 1-3, pp. 209–227, 1997.
[22] J. G. Andrews, F. Baccelli, and R. K. Ganti, "A tractable approach to coverage and rate in cellular networks," *IEEE Trans. Commun.*, vol. 59, pp. 3122–3134, Nov. 2011.
[23] T. D. Novlan, H. S. Dhillon, and J. G. Andrews, "Analytical modeling of uplink cellular networks," *IEEE Trans. Wireless Commun.*, vol. 12, pp. 2669–2679, June 2013.
[24] M. Haenggi, J. G. Andrews, F. Baccelli, O. Dousse, and M. Franceschetti, "Stochastic geometry and random graphs for the analysis and design of wireless networks," *IEEE J. Sel. Areas Commun.*, vol. 27, pp. 1029–1046, July 2009.
[25] K. Huang, "Spatial throughput of mobile ad hoc networks with energy harvesting," *IEEE Trans. Inf. Theory*, vol. 59, pp. 7597–7612, Nov. 2013.
[26] S. Lee, R. Zhang, and K. Huang, "Opportunistic wireless energy harvesting in cognitive radio networks," *IEEE Trans. Wireless Commun.*, vol. 12, pp. 4788–4799, Sept. 2013.
[27] S. Verdu, *Multiuser Detection*. Cambridge University Press, 1998.
[28] T. S. Rappaport, *Wireless Communications: Principles and Practice*. Prentice Hall, 2001.
[29] S. Luo, R. Zhang, and T. J. Lim, "Optimal save-then-transmit protocol for energy harvesting wireless transmitters," *IEEE Trans. Wireless Commun.*, vol. 12, no. 3, pp. 1196–1207, 2013.
[30] F. Baccelli, B. Blaszczyszyn, and P. Muhlethaler, "An ALOHA protocol for multihop mobile wireless networks," *IEEE Trans. Inf. Theory*, vol. 52, pp. 421–36, Feb. 2006.
[31] J. F. C. Kingman, *Poisson Processes*. Oxford University Press, 1993.
[32] S. B. Lowen and M. C. Teich, "Power-law shot noise," *IEEE Trans. Inf. Theory*, vol. 36, pp. 1302–1318, Nov. 1990.
[33] M. Haenggi, "On distances in uniformly random networks," *IEEE Trans. Inf. Theory*, vol. 51, pp. 3584–86, Oct. 2005.
[34] S. P. Weber, J. G. Andrews, X. Yang, and G. de Veciana, "Transmission capacity of wireless ad hoc networks with successive interference cancelation," *IEEE Trans. Inf. Theory*, vol. 53, pp. 2799–2814, Aug. 2007.

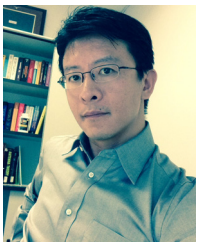

Kaibin Huang (S'05 – M'08 – SM'13) received the B.Eng. (first-class hons.) and the M.Eng. degrees from the National University of Singapore in 1998 and 2000, respectively, and the Ph.D. degree from The University of Texas at Austin (UT Austin) in 2008, all in electrical engineering.

Since Jan. 2014, he has been an assistant professor in the Dept. of Electrical and Electronic Engineering (EEE) at the University of Hong Kong. He is an adjunct professor in the School of EEE at Yonsei University in S. Korea. He used to be a faculty member in the Dept. of Applied Mathematics (AMA) at the Hong Kong Polytechnic University (PolyU) and the Dept. of EEE at Yonsei University. He had been a Postdoctoral Research Fellow in the Department of Electrical and Computer Engineering at the Hong Kong University of Science and Technology from June 2008 to Feb. 2009 and an Associate Scientist at the Institute for Infocomm Research in Singapore from Nov. 1999 to Jul. 2004. His research interests focus on the analysis and design of wireless networks using stochastic geometry and multi-antenna limited feedback techniques.

He frequently serves on the technical program committees of major IEEE conferences in wireless communications. He chairs the Comm. Theory Symp. of IEEE GLOBECOM 2014 and the Adv. Topics in Wireless Comm. Symp. of IEEE/CIC ICCC 2014 and has been the technical co-chair for IEEE CTW 2013, the track chair for IEEE Asilomar 2011, and the track co-chair for IEE VTC Spring 2013 and IEEE WCNC 2011. He is a guest editor for the IEEE JOURNAL ON SELECTED AREAS IN COMMUNICATIONS, an editor for the IEEE TRANSACTIONS ON WIRELESS COMMUNICATIONS, IEEE WIRELESS COMMUNICATIONS LETTERS, and also *IEEE/KICS Journal of Communications and Networks*. He is an elected member of the SPCOM Technical Committee of the IEEE Signal Processing Society. Dr. Huang received the Outstanding Teaching Award from Yonsei, Motorola Partnerships in Research Grant, the University Continuing Fellowship from UT Austin, and Best Paper Awards from IEEE GLOBECOM 2006 and PolyU AMA in 2013.

Vincent K. N. Lau Vincent obtained B.Eng (Distinction 1st Hons) from the University of Hong Kong (1989-1992) and Ph.D. from the Cambridge University (1995-1997). He joined Bell Labs from 1997-2004 and the Department of ECE, Hong Kong University of Science and Technology (HKUST) in 2004. He is currently a Professor and the Founding Director of Huawei-HKUST Joint Innovation Lab at HKUST. His current research focus includes robust cross layer optimization for MIMO/OFDM wireless systems, interference mitigation techniques for wireless networks, delay-optimal cross layer optimizations as well as multi-timescale stochastic network optimization.